

Nonlinear control of speed in a water pumping system powered by PV panels

¹HASSAN ABOUBAIDA, ²MOHAMED CHERKAOU, ³ABDLMONIME EL MAGRI

Department of Electrical Engineering,
Ecole Mohamadia d'ingénieur,
Mohamed V University,
RABAT, MOROCCO

Email: ¹Hassan_abouobaida@yahoo.fr; ²Cherkaoui@emi.ac.ma; ³el_maguri@yahoo.fr

Abstract—The present work describes the analysis, modeling and control of a cascade DC-DC power conditioning stage and AC-DC boost rectifier to control a speed of DC motor in water pumping systems. To maximize energy extracted from PV generator and control speed of DC motor a backstepping controller is designed. The stability of the control algorithm is demonstrated by means of Lyapunov analysis. The achievement of the DC-DC and AC-DC conversion at unity power factor and the efficient PV's energy extraction are validated with simulation results.

Keywords: MPPT, unity power factor, backstepping controller.

1. Introduction

Photovoltaic (PV) is a technology in which the radiant energy from the sun is converted to direct current. The photovoltaic process produces power silently and is completely self-contained, as there are no moving parts. These systems can withstand severe weather conditions including snow and ice. Photovoltaic systems for different applications can be either stand alone or grid connected. In a stand alone system, the load has no connection to the utility grid and often relies on a set of batteries to secure an energy supply at night and other times when the solar panels do not produce electricity. A utility interactive or grid connected system is employed in applications where utility service is already available. In this case, there is no need for battery storage because the power station can be used to supplement photovoltaic generation when the load exceeds the available PV output. The use of photovoltaic as the power source for pumping water is considered as one of the most promising areas of PV application. Photovoltaic powered water pumping systems require only that there be adequate sunshine and a source of water. The use of photovoltaic power for water pumping is appropriate, as there is often a natural relationship between the availability of solar power and the water requirement. The pumped water can be used in many

applications such as domestic use, water for irrigation and village water supplies. The advantages of using water pumps powered by photovoltaic systems include low maintenance, ease of installation, reliability and the matching between the powers generated and the water usage needs.

A power conditioning system linking the solar array and the power DC motor is needed to facilitate an efficient energy transfer between them, this implies that the power stage has to be able to extract the maximum amount of energy from the PV, to assure that the input current presents both low harmonic distortion and to control a speed of DC motor in front of system's perturbations [1].

In order to extract the maximum amount of energy the PV system must be capable of tracking the solar array's maximum power point (MPP) that varies with the solar radiation value and temperature. Several MPPT algorithms have been proposed [2], namely, Perturb and Observe (P&O) [3], incremental conductance [4], fuzzy based algorithms [5], etc. They differ from its complexity and tracking accuracy but they all required sensing the PV current and/or the PV voltage.

Several controller strategies have been used in the literature, citing the PID [6] that is generally suitable

for linear systems, the sliding mode [7] for which the chattering problem, and fuzzy logic adapted to systems without a mathematical model [8].

In this work, the problem of controlling switched power converters is approached using the backstepping technique [9]. While feedback linearization methods require precise models and often cancel some useful nonlinearities, backstepping designs offer a choice of design tools for accommodation of uncertain nonlinearities and can avoid wasteful cancellations [10]. The backstepping approach is applied to a specific class of switched power converters, namely dc-to-dc converters. In the case where the converter model is fully known the backstepping nonlinear controller is shown to achieve the control objectives i.e. input voltage tracking and speed control of DC motor with respect to climate change and load torque.

The desired array voltage is designed online using a P&O (Perturb and Observe) MPP tracking algorithm [8]. The proposed strategy ensures that the MPP is determined, the speed of DC motor is controlled to its reference value and the close loop system will be asymptotically stable. The stability of the control algorithm is verified by Lyapunov analysis [9].

The rest of the paper is organized as follows. The dynamic model of the global system is described in Section 2. A backstepping controller is designed along with the corresponding closed-loop error system and the stability analysis is discussed in Section 3. In Section 4, a simulation results proves the effectiveness of this approach with respect solar radiation, temperature, load torque and speed changes.

2. MPPT System Modeling

The solar generation model consists of a PV array module, dc-to-dc boost converter, ac-to-dc boost rectifier and dc-to-dc buck converter as shown in Figure 1.

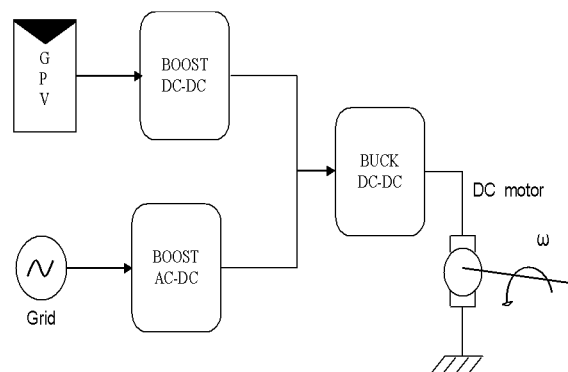


Fig.1. Power conversion structure of water pumping system

2.1 PV model

PV array is a p-n junction semiconductor, which converts light into electricity. When the incoming solar energy exceeds the band-gap energy of the module, photons are absorbed by materials to generate electricity. The equivalent-circuit model of PV is shown in Figure 2. It consists of a light-generated source, diode, series and parallel resistances [11]-[12].

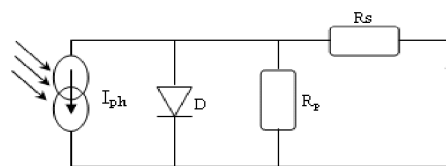


Fig.2. Equivalent model of solar cell

2.4 BOOST model

The dynamic model of the power boost converter presented in figure 3 can be expressed by an instantaneous switched model as follows [10]:

$$c_1 \cdot \dot{u}_{pv} = i_{pv} - i_{L1} \quad (1)$$

$$L_1 \cdot \dot{i}_{L1} = u_{pv} - (1 - u_1) \cdot u_{dc} \quad (2)$$

where L_1 and i_{L1} represents the dc-to-dc converter storage inductance and the current across it, u_{dc} is the DC bus voltage and u_1 is the switched control signal that can only take the discrete values 0 (switch open) and 1 (switch closed).

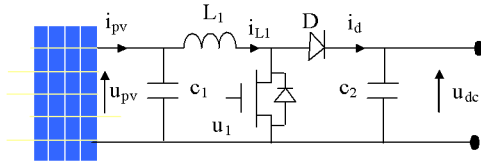


Fig.3. PV array connected to boost converter

Using the state averaging method, the switched model can be redefined by the average PWM model as follows:

$$c_1 \cdot \dot{u}_{pv} = i_{pv} - i_{L1} \quad (3)$$

$$L \cdot \dot{i}_L = u_{pv} - \alpha_1 \cdot u_{c2} \quad (4)$$

Where α_1 is averaging value of u_1-1 , u_{pv} and i_{pv} are the average states of the output voltage and current of the solar cell, i_{L1} is the average state of the inductor current.

2.4 Boost rectifier model

The active power transfer from the grid is accomplished by power factor correction (line current in phase with grid voltage). The rectifier operates as a current-control rectifier. Noticing that u_2 stand for the control signal of boost rectifier, the system can be represented by differential equations [3]:

$$c_4 \cdot \dot{u}_{c4} = i_s - i_b \quad (5)$$

$$L_g \cdot \dot{i}_g = u_g - u_{c3} \quad (6)$$

$$u_e = (2 \cdot u_2 - 1) \cdot u_s \quad (7)$$

$$i_s = (2 \cdot u_2 - 1) \cdot i_e \quad (8)$$

$$c_3 \cdot \dot{u}_{c3} = i_g - i_e \quad (9)$$

$$L_2 \cdot \dot{i}_e = u_{c3} - u_e \quad (10)$$

Where u_{c4} , i_g , u_g designs a DC voltage, input rectifier current and AC grid voltage respectively. And i_s , i_b , i_g are output rectifier current, output DC current and grid current respectively.

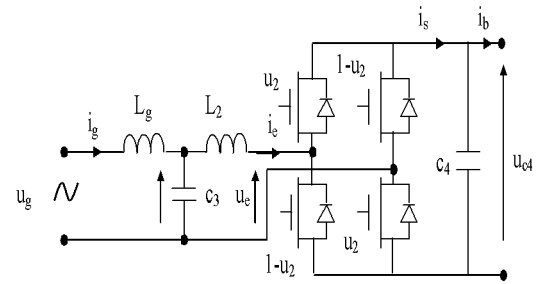


Fig.4. boost rectifier operate as PFC converter connected to DC bus

Using the state averaging method (on cutting period), the switched model can be redefined by the average PWM model as follows:

$$c_4 \cdot \dot{u}_{c4} = i_s - i_b \quad (11)$$

$$L_g \cdot \dot{i}_g = u_g - u_{c3} \quad (12)$$

$$u_e = \alpha_2 \cdot u_s \quad (13)$$

$$i_s = \alpha_2 \cdot i_e \quad (14)$$

$$c_3 \cdot \dot{u}_{c3} = i_g - i_e \quad (15)$$

$$L_2 \cdot \dot{i}_e = u_{c3} - u_e \quad (16)$$

Where α_2 is averaging value of $(1 - u_2)$

2.4 Buck converter model

The power converter here is like buck. It provides power to the DC machine with a share of power supplied by the photovoltaic generator and the rest by the power supplied by the grid source. The studied converter accomplish constant speed operation of the DC machine to ensure a constant flow of water pumping. Figure 5 illustrate a buck converter connected to DC motor. Noticing that u_3 stand for the control signal of buck converter, the system can be represented by differential equations [3]:

$$J \cdot \dot{\Omega} = k \cdot i_m - f \cdot \Omega - T_L \quad (13)$$

$$L \cdot \dot{i}_m = u_3 \cdot u_{dc} - k \cdot \Omega - R_m \cdot i_m \quad (14)$$

Where u_{dc} , u_m designs a DC voltage, output buck converter voltage respectively. And i_{dc} , i_m are

converter input current and DC motor current respectively. L , Ω , T_L are the addition of DC motor inductor and the dc-to-dc converter storage inductance, rotor speed and the load torque respectively and α_3 is the averaging value of u_3 .

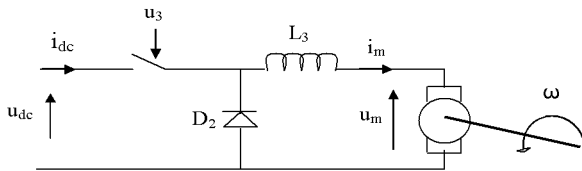


Fig.5. buck converter connected to DC motor

Using the state averaging method (on cutting period), the switched model of buck converter can be redefined by the average PWM model as follows:

$$J \cdot \dot{\Omega} = k \cdot i_m - f \cdot \Omega - T_L \quad (15)$$

$$L \cdot \dot{i}_m = \alpha_3 \cdot u_{dc} - k \cdot \Omega - R_m \cdot i_m \quad (16)$$

Where α_3 is averaging value of u_3

3. Nonlinear controller Design

Two main objectives have to be fulfilled in order to transfer efficiently the photovoltaic generated energy into the DC motor are tracking the PV's maximum power point (MPP) and obtain unity power factor at the input grid current and control speed of DC motor. Figure 6 shows the control scheme used to accomplish the previous objectives.

3.1 Backstepping controller to track MPPT

The boost converter is governed by control signal α_1 generated by a backstepping controller 1 that allow to extract maximum of photovoltaic generator control by regulating the voltage of the photovoltaic generator to its reference provided by conventional P&O MPPT algorithm.

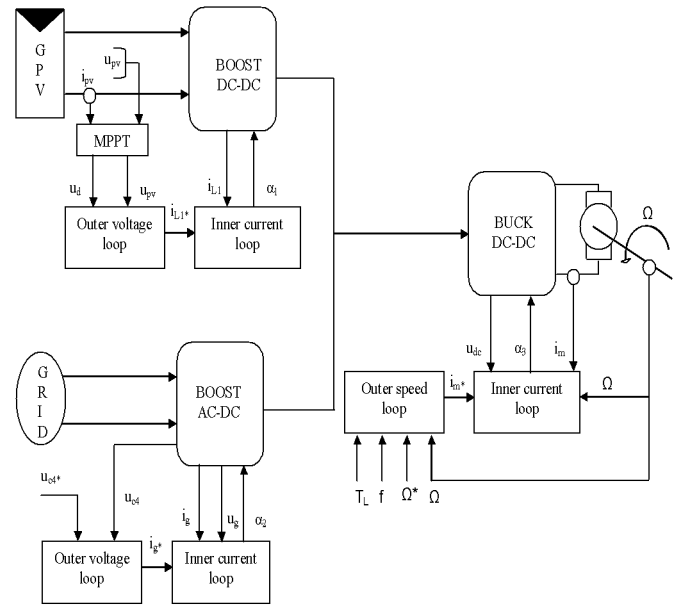


Fig.6 Control scheme for boost converter, PFC rectifier and buck converter with control speed

Step 1. Let us introduce the input error:

$$e_1 = u_{pv} - u_{pv}^* \quad (17)$$

Deriving e_1 with respect to time and accounting for (3), implies:

$$\dot{e}_1 = \dot{u}_{pv} - \dot{u}_{pv}^* = \left(\frac{i_{pv}}{c_1} - \frac{i_{L1}}{c_1} \right) - \dot{u}_{pv}^* \quad (18)$$

In equation (18), i_{L1} behaves as a virtual control input. Such an equation shows that one gets $\dot{e}_1 = -k_1 \cdot e_1$ ($k_1 > 0$ being a design parameter) provided that:

$$i_{L1} = k_1 \cdot c_1 \cdot e_1 + i_{pv} - c_1 \cdot \dot{u}_{pv}^* \quad (19)$$

As i_{L1} is just a variable and not (an effective) control input, (18) cannot be enforced for all $t \geq 0$. Nevertheless, equation (19) shows that the desired value for the variable i_{L1} is:

$$\alpha_1 = i_{L1}^* = k_1 \cdot c_1 \cdot e_1 + i_{pv} - c_1 \cdot \dot{u}_{pv}^* \quad (20)$$

Indeed, if the error:

$$e_2 = i_{L1} - i_{L1}^* \quad (21)$$

vanishes (asymptotically) then control objective is achieved i.e. $e_1 = u_{pv} - u_{pv}^*$ vanishes in turn. The desired value α_1 is called a stabilization function.

Now, replacing i_{L1} by $(e_2 + i_{L1}^*)$ in (18) yields:

$$\dot{e}_1 = \left(\frac{i_{pv}}{c_1} - \frac{i_{L1}^* + e_2}{c_1} \right) - \dot{u}_{pv}^* \quad (22)$$

which, together with (20), gives:

$$\dot{e}_1 = -k_1 \cdot e_1 - \frac{e_2}{c_1} \quad (23)$$

Step 2. Let us investigate the behaviour of error variable e_2 .

In view of (4) and (21), time-derivation of e_2 turns out to be:

$$\dot{e}_2 = \dot{i}_{L1} - \dot{i}_{L1}^* = \frac{u_{pv}}{L_1} - \frac{\alpha \cdot u_{c2}}{L_1} - \dot{i}_{L1}^* \quad (24)$$

From (20) one gets:

$$\dot{\alpha}_1 = \dot{i}_{L1}^* = k_1 \cdot c_1 \cdot \dot{e}_1 + \dot{i}_{pv} - c_1 \cdot \ddot{u}_{pv}^* \quad (25)$$

which together with (24) implies:

$$\dot{e}_2 = \frac{u_{pv}}{L_1} - \frac{\alpha \cdot u_{c2}}{L_1} - k_1 \cdot c_1 \cdot \dot{e}_1 - \dot{i}_{pv} + c_1 \cdot \ddot{u}_{pv}^* \quad (26)$$

In the new coordinates (e_1, e_2) , the controlled system in (3) and (4) is expressed by the couple of equations (23) and (26). We now need to select a Lyapunov function for such a system. As the objective is to drive its states (e_1, e_2) to zero, it is natural to choose the following function:

$$v = \frac{1}{2} \cdot e_1^2 + \frac{1}{2} \cdot e_2^2 \quad (27)$$

The time-derivative of the latter, along the (e_1, e_2) trajectory, is:

$$\dot{v} = e_1 \cdot \dot{e}_1 + e_2 \cdot \dot{e}_2 \quad (28)$$

$$\dot{v} = -k_1 \cdot e_1^2 - k_2 \cdot e_2^2 + e_2 \cdot \left[\frac{u_{pv}}{L_1} - \frac{\alpha \cdot u_{c2}}{L_1} - k_1 \cdot c_1 \cdot \dot{e}_1 - \frac{e_1}{c_1} - \dot{i}_{pv} + c_1 \cdot \ddot{u}_{pv}^* + k_2 \cdot e_2 \right] \quad (29)$$

where $k_2 > 0$ is a design parameter and \dot{e}_2 is to be replaced by the right side of (26). Equation (29) shows that the equilibrium $(e_1, e_2) = (0, 0)$ is globally asymptotically stable if the term between brackets in (29) is set to zero. So doing, one gets the following control law:

$$\alpha_1 = \frac{L_1}{u_{c2}} \left[\frac{u_{pv}}{L_1} + k_1 \cdot c_1 \cdot \dot{e}_1 - \frac{e_1}{c_1} - \dot{i}_{pv} + c_1 \cdot \ddot{u}_{pv}^* + k_2 \cdot e_2 \right] \quad (30)$$

Proposition 1:

Consider the control system consisting of the average PWM Boost model (3)-(4) in closed-loop with the controller (29), where the desired input voltage reference u_{pv}^* is sufficiently smooth and satisfies $u_{pv}^* > 0$. Then, the closed loop system errors (e_1, e_2) achieve globally asymptotically.

3.2 Speed controller design

This controller consists of an inner current loop and an outer speed loop. The inner current loop is responsible to regulate the current of DC motor. The outer loop assures a steady-state control a speed of DC motor [3].

Step 1. Let us introduce the input error:

$$e_3 = \Omega - \Omega^* \quad (31)$$

Where Ω^* is a derivable reference signal of speed of DC motor. Deriving e_3 with respect to time and accounting for (15) implies:

$$\dot{e}_3 = \dot{\Omega} - \dot{\Omega}^* = \frac{k \cdot i_m}{J} - \frac{f \cdot \Omega}{J} - \frac{T_L}{J} - \dot{\Omega}^* \quad (32)$$

Where i_m is a virtual control input. Such an equation shows that one gets $\dot{e}_3 = -k_3 \cdot e_3$ ($k_3 > 0$ being a design parameter) provided that:

$$i_m^* = \frac{f \cdot \Omega}{k} + \frac{T_L}{k} - \frac{J \cdot k_3 \cdot e_3}{k} \quad (33)$$

As i_m is just a variable (not effective) control input, equation (33) cannot be enforced for all $t \geq 0$. Indeed, a new error is introduced:

$$e_4 = i_m - i_m^* = i_m - \left(\frac{f \cdot \Omega}{k} + \frac{T_L}{k} - \frac{J \cdot k_3 \cdot e_3}{k} \right) \quad (34)$$

vanishes (asymptotically) then control objective is achieved i.e. $e_3 = \Omega - \Omega^*$ vanishes in turn. The desired value i_m^* is called a stabilization function.

Now, replacing i_m by $(i_m^* + e_4)$ in (32) yields:

$$\dot{e}_3 = \frac{k \cdot (i_m^* + e_4)}{J} - \frac{f \cdot \Omega}{J} - \frac{T_L}{J} - \dot{\Omega}^* \quad (35)$$

which, together with (32), gives:

$$\dot{e}_3 = -k_3 \cdot e_3 + \frac{k \cdot e_4}{J} \quad (36)$$

Step 2. Let us investigate the behavior of error variable e_4 .

In view of (16), time-derivation of e_4 turns out to be:

$$\dot{e}_4 = \dot{i}_m - \dot{i}_m^* = \frac{\alpha_3 \cdot u_{dc}}{L} - \frac{k \cdot \Omega}{L} - \frac{R_m \cdot i_m}{L} - \dot{i}_m^* \quad (37)$$

From (33) one gets:

$$\dot{i}_m^* = \frac{f \cdot \dot{\Omega}}{k} + \frac{\dot{T}_L}{k} - \frac{J \cdot k_3 \cdot \dot{e}_3}{k} \quad (38)$$

Substituting (38) in (37) implies:

$$\dot{e}_4 = \dot{i}_m - \dot{i}_m^* = \frac{\alpha_3 \cdot u_{dc}}{L} - \frac{k \cdot \Omega}{L} - \frac{R_m \cdot i_m}{L} - \left(\frac{f \cdot \dot{\Omega}}{k} + \frac{\dot{T}_L}{k} - \frac{J \cdot k_3 \cdot \dot{e}_3}{k} \right) \quad (39)$$

In the new coordinates (e_3, e_4) , the controlled system is expressed by the couple of equations (36) and (39). We now need to select a Lyapunov function for such a system. As the objective is to drive its states (e_3, e_4) to zero, it is natural to choose the following function:

$$v = \frac{1}{2} \cdot e_3^2 + \frac{1}{2} \cdot e_4^2 \quad (40)$$

The time-derivative of the latter, along the (e_3, e_4) trajectory is:

$$\begin{aligned} \dot{v} &= e_3 \cdot \dot{e}_3 + e_4 \cdot \dot{e}_4 \\ \dot{v} &= -k_3 \cdot e_3^2 - k_4 \cdot e_4^2 \\ &+ e_4 \cdot \left[k_4 \cdot e_4 + \frac{e_3 \cdot k}{J} + \frac{\alpha_3 \cdot u_{dc}}{L} - \frac{k \cdot \Omega}{L} \right. \\ &\quad \left. - \frac{R_m \cdot i_m}{L} - \left(\frac{f \cdot \dot{\Omega}}{k} + \frac{\dot{T}_L}{k} - \frac{J \cdot k_3 \cdot \dot{e}_3}{k} \right) \right] \end{aligned} \quad (41)$$

where $k_4 > 0$ is a design parameter and i_m^* is to be replaced by the right side of (38). Equation (41) shows that the equilibrium $(e_3, e_4) = (0, 0)$ is globally asymptotically stable if the term between brackets in (41) is set to zero. So doing, one gets the following control law:

$$\begin{aligned} \alpha_3 &= \frac{k \cdot \Omega + R_m \cdot i_m - L \cdot k_2 \cdot e_2 - \frac{e_3 \cdot k \cdot L}{J}}{u_{dc}} \\ &+ \frac{L \cdot f \cdot \dot{\Omega} + L \cdot \dot{T}_L - L \cdot k \cdot k_4 \cdot e_4 - L \cdot J \cdot k_3 \cdot \dot{e}_3}{k \cdot u_{dc}} \end{aligned} \quad (42)$$

Proposition 2:

Consider the control system consisting of the average PWM Buck model in closed-loop with the controller (42), where the desired speed motor reference Ω^* is sufficiently smooth. Then, the closed loop system errors (e_3, e_4) achieve globally asymptotically.

3.3 Control of Boost rectifier

To obtain unity power factor at the input grid current and regulate the DC bus voltage, the AC-DC converter is introduced. The control of this converter is to use two control loops. The inner loop ensure the output current of the grid so that it is in phase with the grid voltage and the external loop to regulate the DC bus voltage to its reference (must be higher than the grid voltage) [13]. Figure 7 shows the approach to achieve the above objectives:

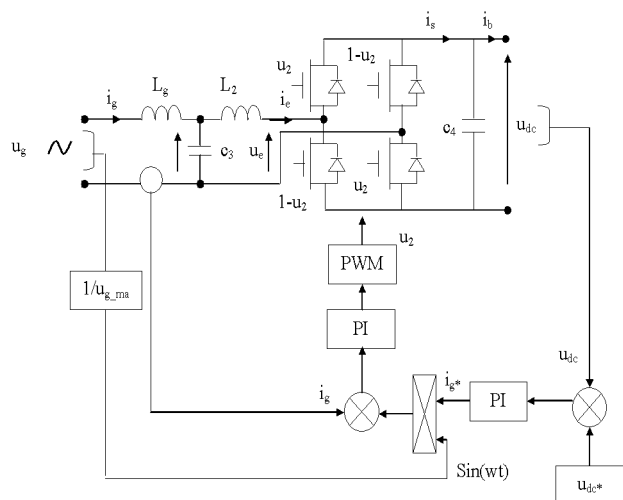


Fig.7. Control scheme of boost rectifier

TABLE
MAIN CHARACTERISTICS OF THE PV SYSTEM

Parameters		Value
PV generator	P_{max}	60W
	u_{pv}	16V
	P_{max}	21.5V
	V_{oc}	3.8A
	I_{cc}	
Boost converter	C_1	220 μ F
	L_1	0.004H
Boost rectifier	L_2	0.001H
	c_2	10 μ F
	u_g	220/50Hz
Buck converter and load	L_3	0.002H
	R_m	0.47 Ω
	L_m	0.0068H
Backstepping Controller	k_1	150
	k_2	10
	k_3	1000
	k_4	150000

4. Simulation result

The PV model, boost rectifier, boost and buck DC-DC converter, DC motor model and backstepping controller are implemented in Matlab/Simulink as illustrated in Figure 6. In the study, RSM-60 PV module has been selected as PV power source in cooperation with grid source, and the parameter of the PV source are chosen to deliver maximum 1kW of power generated by connecting 16 module of RSM-60 parallelly. The specification of the system and PV module are respectively summarized in the following table.

Matlab® simulation of the complete water pumping system with the backstepping controller and the MPPT algorithm has been carried out using the following parameters:

- switching frequency = 25kHz

The water pumping system is evaluated on two aspects: the first one is the ability to regulate the speed of DC motor to a reference chosen by the user when the solar radiation changes. The second one is the ability to absorb a current from the grid with a power factor near unity.

Figure 8.a, 8.b show the step irradiance input 500 to 1000 W/m² under the same temperature (T=25 °C), the temperature step from 25°C to 35°C at time 3s respectively. The load torque variation is illustrated in figure 8.c. figure 7.d shows the PV voltage properly following its reference provided by the MPPT algorithm.

Figure 8.e illustrates the maximum power extracted from the solar panel according to a step in solar radiation from 500 to 1000 w/m². This power limits the power demand of the grid and ensure a constant DC bus voltage as possible. Figure 8.f shows the DC bus voltage well achieved to its reference (450v). The DC bus voltage reaches its reference value at t=0.5s and is kept there until the end of simulation. Figure 9.a shows the speed of DC motor follows its reference (50rad / s) after a smooth transient response. This speed reaches the desired value in 0.8s.

figure 9.b and 9.c illustrates the current and the voltage absorbed from the grid. Notice that the grid current is in phase with the AC voltage (unity power factor) and the current electric system demand

decreases when solar radiation increases from 500 to 1000 w/m². The simulation results prove the robustness of the studied controller with response of the irradiation, temperature and the load torque changes.

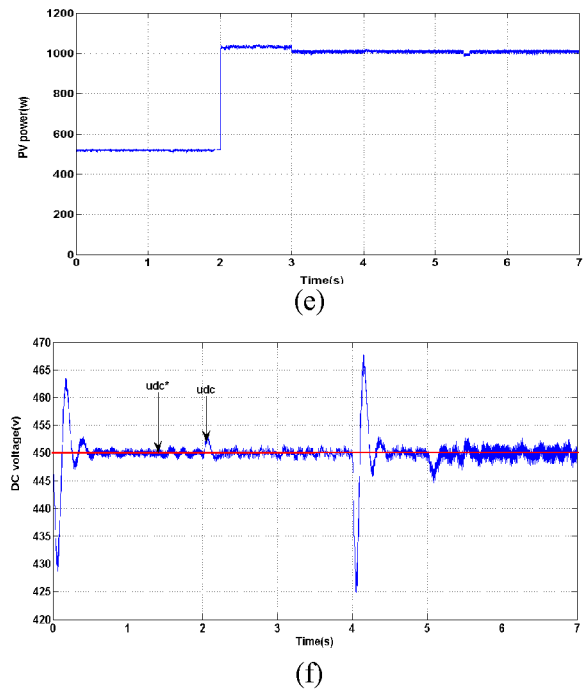
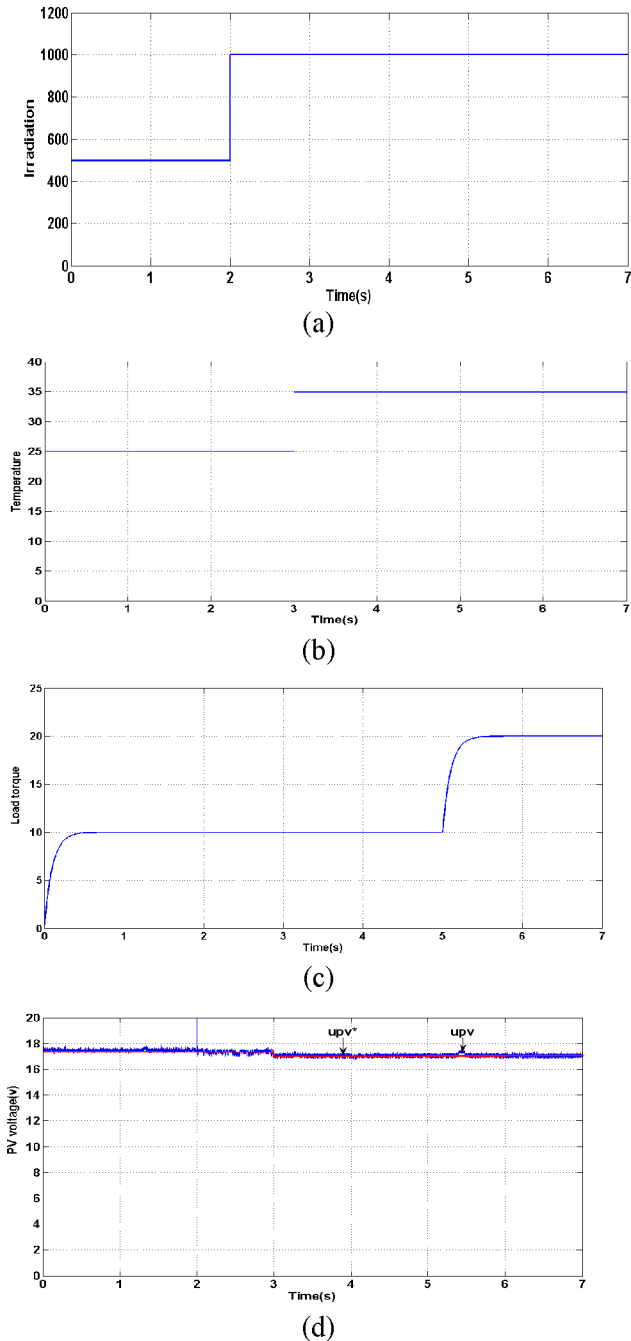
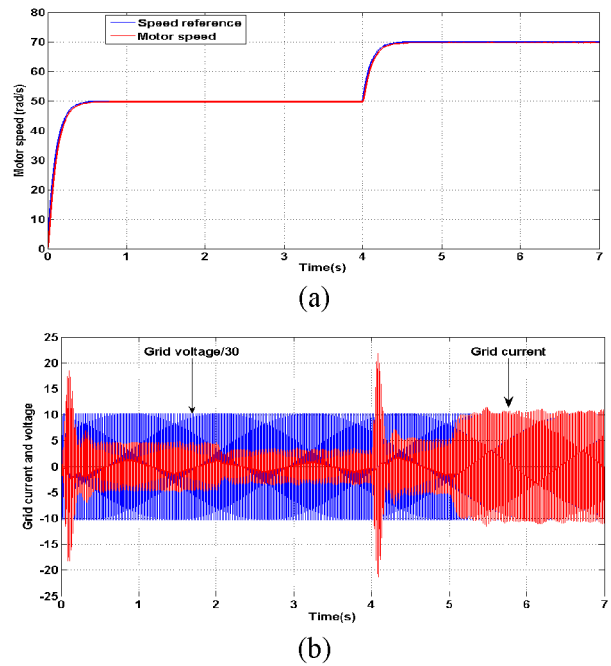


Figure 8. (a) radiation, (b) Temperature, (c) Load torque, (d) PV voltage, (e) PV power, (f) DC voltage



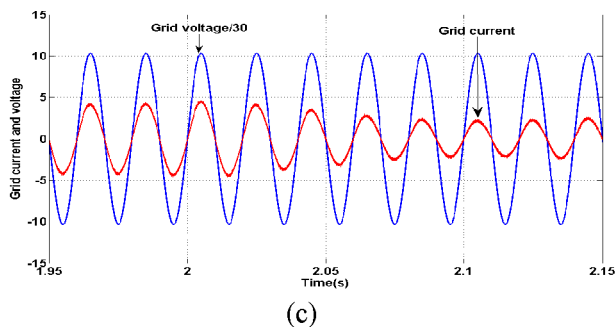


Figure.9. (a) Speed of DC motor and reference, (b) Grid voltage and current, (f) Grid voltage and current [1.95 to 2.15s]

5. Conclusions

A backstepping control strategy has been developed for a solar generating system to extract the power from a photovoltaic panel, assure an unitary power factor and regulate the speed of DC motor in varying weather conditions. A desired array voltage is designed online using an MPPT searching algorithm to seek the unknown optimal array voltage. To track the designed trajectory, a tracking controller is developed to modulate the duty cycle of the boost-buck converter. The proposed controller is proven to yield global asymptotic stability with respect to the tracking errors via Lyapunov analysis. Simulation results prove the robustness of the nonlinear controller with respect the load torque and the weather changes.

References:

- [1] A.A. Ghoneim, Design optimization of photovoltaic powered water pumping systems, *Energy Conversion and Management*, 2006, pp. 1449–1463
- [2] Trishan Esham, Patrick L. Chapman, Comparison of Photovoltaic Array Maximum Power Point Tracking Techniques, *IEEE Transaction on Energie Conversion*, Vol. 22, No. 2, June 2007, pp. 439 - 449
- [3] N. Femia, G. Petrone, G. Spagnuolo, and M. Vitelli, "Optimization of Perturb and Observe maximum power point tracking method", *IEEE Transactions on Power Electronics*, Vol. 20, n. 4, July 2005, pp. 963–973
- [4] Safari, A.; Mekhilef, S., Simulation and Hardware Implementation of Incremental Conductance MPPT With Direct Control Method Using Cuk Converter, *IEEE Transactions on Industrial Electronics*, April 2011, Vol 58, pp. 1154 - 1161
- [5] Chim, C.S.; Neelakantan, P.; Yoong, H.P.; Teo, K.T.K.; Fuzzy Logic Based MPPT for Photovoltaic Modules Influenced by Solar Irradiation and Cell Temperature, *13th International Conference on Computer Modelling and Simulation*, 2011, pp. 376 - 381
- [6] Chen-Chi Chu , Chieh-Li Chen, " Robust maximum power point tracking method for photovoltaic cells: A sliding mode control approach ", *Solar Energy*, Volume 83, 2009, pp 1370-1378
- [7] Liping Guo; Implementation of digital PID controllers for DC-DC converters using digital signal processors, *IEEE International Conference on Electro/Information Technology*, 2007, pp. 306 - 311
- [8] H. Abouobaida, M. Cherkaoui, "Robust controller for interleaved DC-DC converters and buck inverter in Grid-Connected Photovoltaic Systems", *WSEAS TRANSACTIONS on POWER SYSTEMS*, Issue. 1, Vol. 6, Jan 2011, pp. 21-30
- [9] Khalil, H. K., *Nonlinear Systems, 2nd ed., Prentice Hall, New York, USA*, 1996
- [10] H. Abouobaida, M. Cherkaoui, Ripple correlation MPPT and Robust Controller for Grid-Connected Photovoltaic Systems, *journal of electrical engineering*, Vol. 11, sept 2011, pp. 116-121
- [11] TAMER T.N. KHATIB, A. MOHAMED and N. AMIN, An Efficient Maximum Power Point Tracking Controller for Photovoltaic Systems Using New Boost Converter Design and Improved Control Algorithm, *WSEAS TRANSACTIONS on POWER SYSTEMS*, Issue 2, Volume 5, April 2010, pp. 53 – 63
- [12] Salima Kebaili, Achour Betka; Design and Simulation of Stand Alone Photovoltaic Systems, *WSEAS TRANSACTIONS on POWER SYSTEMS*, Issue 4, Volume 6, October 2011, pp. 89-99
- [13] Nicolas BERNARD, Bernard MUL TON, Hamid BEN AHMED, Le redresseur MLI en absorption sinusoidale de courant, *Revue 3EI n.35* Décembre 2003, pp. 56-65



Hassan Abouobaida was born in Rabat, Morocco, in 1974. He received the « Diplôme d'ENSET » in Electrical Engineering from Ecole Normal Supérieur de l'Enseignement Technique, Mohamedia in 1998, and the « Diplôme DESA », in Electrical Engineering from Ecole Mohamadia d'Ingénieur, Université Mohamed V, Rabat, Morocco in 2007. He is currently teacher in IBN SINA Technical School, Kenitra, Morocco. His research interests power electronics, control systems and renewable energy.



Mohamed Cherkaoui was born in Marrakech, Morocco, in 1954. He received the diplôme d'ingénieur d'état degree from the Ecole Mohammadia, Rabat, Morocco, in 1979 and the M.Sc.A. and Ph.D. degrees from the Institut National Polytechnique de la Lorraine, Nancy, France, in 1983 and 1990, respectively, all in Electrical Engineering. During 1990-1994, he was a Professor in Physical department, cadi Ayyad university, Marrakech, Morocco. In 1995, he joined the Department of Electrical Engineering, Ecole Mohammadia, Rabat, Morocco, where is currently a Professor and University Research Professor. His current research interests include renewable energy, motor drives and power system. Dr. Cherkaoui is a member of the IEEE.